Why Does Enzyme Not Leach from Metal−Organic Frameworks (MOFs)? Unveiling the Interactions between an Enzyme Molecule and a MOF

Yao Chen, Sungyub Han, Xiao Li,* Zhenjie Zhang, and Shengqian Ma*

Department of Chemistry, University of South Florida, 4202 East Fowler Avenue, Tampa, Florida 33620, United States

S *Supporting Information*

ABSTRACT: The strong interactions between microperoxidase (MP-11) and Tb-mesoMOF were identified via Raman spectroscopic studies, which revealed that MP-11 molecules interact with the framework of Tb-mesoMOF through $\pi\cdots\pi$ interactions between the heme of MP-11 and the conjugated triazine and benzene rings in the organic ligand of Tb-mesoMOF. The strong interactions facilitate the retention of MP-11 molecules within the metal−organic framework (MOF) pores, which is in striking contrast with the severe leaching of MP-11 from MCM-41 due to the lack of specific interactions between enzyme molecules and the mesoporous silica material.

Enzymes are known to be the most sophisticated catalysts designed by nature because of their high efficiency and high stereo-, chemo-, and regioselectivity. Generally, enzymatic catalysis is more environmentally friendly and features shorter synthetic routes. These merits have prompted the persistent exploration of employing enzymes for the chemical, pharmaceutical, and food industries.[1,2] However, the industrial application of enzymes in those fields is usually hampered by their low operational stability, difficult recovery, and lack of reusability.[1−3] This necessitates the development of materials and methods that can effectively stabilize enzymes in what is often an unnatural environment while retaining their functions and activities, and immobilizing enzymes on solid supports presents the advantages of enhanced stability as well as ease of separation and facile recovery for reuse.[4] Among the various types of host matrix materials for enzyme immobilization, mesoporous silica materials have mostly been investigated,[5] but they often suffer from leaching of the immobilized enzyme during the reaction process, which in return results in a loss of activity upon reuse.

Recently, we demonstrated the successful immobilization of the enzyme microperoxidase-11 (MP-11) and a series of other heme proteins into a mesoporous metal−organic framework (mesoMOF), and the enzyme@mesoMOF materials demonstrated superiority in enzymatic catalysis compared to the mesoporous silica material counterparts.[6] Our studies indicated that the enzyme molecules can be retained inside mesoMOF for a long period of time without leaching, whereas severe leaching was observed for mesoporous silica materials (Figure S1 in the Supporting Information, SI). Then the question is, why does enzyme not leach from the MOF but from the mesoporous silica material? We speculate that the ability of the MOF to retain the

enzyme is due to strong interactions between the organic components of the framework and enzyme molecules, whereas the lack of specific interactions between the enzyme molecules and mesoporous silica materials could account for the escape of enzyme from the support.

To unveil the interactions between the enzyme molecules and mesoMOF framework, herein we present Raman spectroscopic studies on MP-11@Tb-mesoMOF (Scheme S1 in the SI) recently developed in our laboratory, which not only exhibited superior enzymatic catalysis performances compared to the MP-11@MCM-41 silica counterpart but also could hold the enzyme molecules without leaching during catalytic assays. These mechanistic studies are fundamentally important because they will provide insightful information regarding how mesoMOFs can stabilize enzymes and/or boost their activities in the heterogeneous catalytic systems, which will help in the design of new functional mesoMOFs for enzyme immobilization with enhanced biocatalysis performances.

Raman spectroscopy, as one of the most important vibrational spectroscopies, has been widely used for various fields because of its advantages such as nondestructive, quick sample preparation and simple data analysis.[7] The Raman studies on chemical compounds allow for both quantitative and qualitative analysis of the chemical structures and have been extensively applied to study the intermolecular interactions of various biomolecules including complicated systems involving cancer cells, hemoglobin, and hormones.[8] It was also demonstrated to successfully investigate the reaction mechanism and dynamic in hemoproteins[8c,9] and detect molecules adsorbed on porous materials.[9] Recently, Raman spectroscopy has been utilized to study gas molecules adsorbed in MOFs,[10] and the success of those studies encouraged us to employ this tool to investigate the interactions between biomolecules and MOF frameworks. In this contribution, we report the employment of Raman spectroscopy to unravel how MP-11 molecules interact strongly with the mesoporous MOF of Tb-mesoMOF, thus avoiding leaching from the MOF, in striking contrast with the mesoporous silica material of MCM-41.

Tb-mesoMOF represents an excellent platform for enzyme immobilization because of its water stability and mesoporous cage structure.[11] It is formed by the coordination of Tb ions and a trigonal-planar ligand, 4,4′,4″-*s*-triazine-2,4,6-triyltribenzoate (TATB), and exhibits a zeolite-like network with two types of

nanoscopic cages of 3.9 and 4.7 nm diameter. In this study, MP-11 was immobilized into Tb-mesoMOF and MCM-41 according to the procedures reported in our previous work.[6a] The afforded MP-11@Tb-mesoMOF and MP-11@MCM-41 were placed in a pH 7.5 4-(2-hydroxyethyl)-1-piperazineethanesulfonic acid (HEPES) buffer for Raman spectral measurements using a confocal Raman microscope and compared with the MP-11, MCM-41, and Tb-mesoMOF frameworks in the same buffer.

In order to obtain optimal intensities of the samples, different exposure times were applied for the Raman measurements: 5 s for the buffer solution and Tb-mesoMOF, 10 s for MP-11@Tb-mesoMOF, 15 s for the MP-11 sample, and 30 s for MP-11@MCM-41. All of the samples were tested in the same HEPES buffer; therefore, the effect of solvation in HEPES on the vibrational modes was taken into consideration. Before measurements of MP-11@Tb-mesoMOF and MP-11@MCM-41, the Raman spectra of the HEPES buffer (red) and MP-11 dissolved in the HEPES buffer (black) were collected between 400 and 1800 cm^{-1}. As shown in Figure S2 in the SI, strong Raman bands belonging to the buffer solution are observed in the spectrum of the MP-11 solution. In addition, the fingerprint vibrational modes of MP-11 can be clearly identified at 1172 cm^{-1} (ν_{30} of heme), 1317 cm^{-1} (ν_{21} of heme), 1374 cm^{-1} (ν_4 of heme), 1567 cm^{-1} (ν_{19} of heme), 1596 cm^{-1} (ν_{37} of heme), and 1644 cm^{-1} (ν_{10} of heme).[9b,13] According to Figures S2 and S4 in the SI, the peak positions of MP-11 dissolved in HEPES and D$_2$O are located at the exact same wavenumbers. This confirms that there are no strong interactions between MP-11 and the HEPES buffer. In order to convince the frequency shifts, we used the HEPES solution of the complex as an internal standard. Figure S5 in the SI shows Raman spectra of HEPES and MP-11@Tb-mesoMOF. The spectra of HEPES above MP-11@Tb-mesoMOF were collected by changing the confocal distance after Raman measurements of MP-11@Tb-mesoMOF.

Figure 1 shows the Raman spectra of MP-11@Tb-mesoMOF, Tb-mesoMOF, and MP-11 in the HEPES buffer. HEPES in the Tb-mesoMOF sample was used as the internal standard shown in Figure S5 in the SI. It is notable that, because confocal Raman microscopy was used during the measurements, the laser was focused on the MP-11@Tb-mesoMOF crystal at the bottom of the cuvette. Therefore, even with the presence of the MP-11@Tb-mesoMOF and Tb-mesoMOF crystals in the pH 7.5 HEPES buffer, only a small amount of the HEPES solution was within the focus volume of the laser. Thus, no strong signal was observed from the HEPES buffer. It can be clearly seen that the Raman spectrum of MP-11@Tb-mesoMOF exhibits the characteristic bands from both MP-11 and Tb-mesoMOF, indicating the presence of MP-11 in Tb-mesoMOF. For example, the peak at 1371 cm^{-1} (dotted line in Figure 1a) assigned to ν_4(C–N) of the heme of MP-11 was observed in the spectra of both MP-11 and MP-11@Tb-mesoMOF. Interestingly, significant energy shifts of the Raman bands of MP-11 were found in MP-11@Tb-mesoMOF. As shown in Figure 1b, the six vibrational bands of MP-11 at 1172, 1317, 1374, 1567, 1596, and 1644 cm^{-1} were red-shifted to 1167, 1311, 1371, 1556, 1577, and 1636 cm^{-1}, respectively, for MP-11@Tb-mesoMOF. The red shift of the last two peaks at 1577 and 1636 cm^{-1} was observed previously[13] and is due to disruption of the dimer or oligomer structure of MP-11, which exists in high concentration when encapsulated into the pores. Considering that the dimensions of MP-11 are ca. 3.3 × 1.7 × 1.1 nm and the sizes of two types of cages in Tb-mesoMOF are 3.9 and 4.7 nm, this suggests that only the monomer form of MP-11 should be accommodated within Tb-mesoMOF. The red
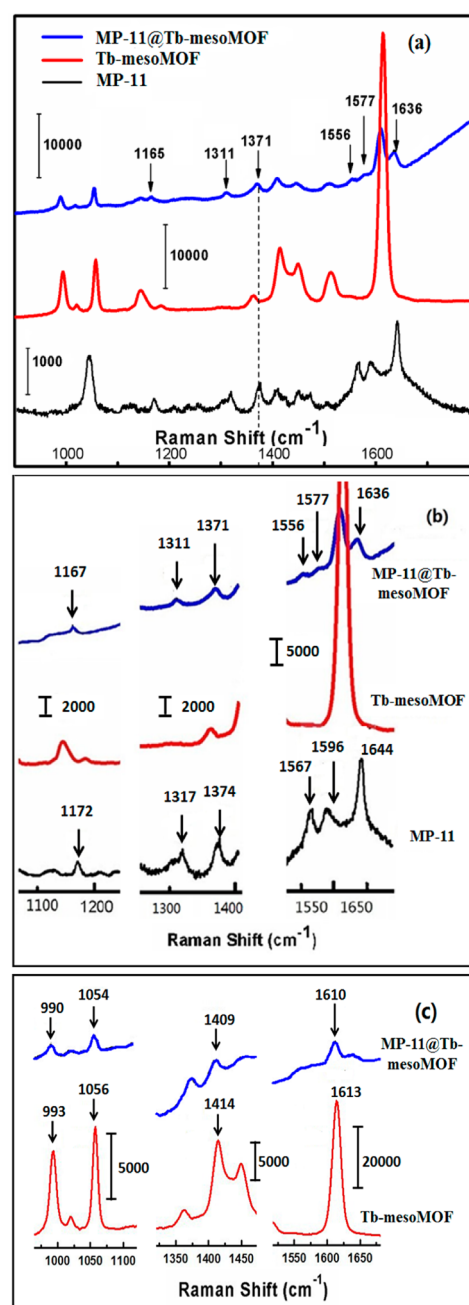
Figure 1. (a) Raman spectra of MP-11@Tb-mesoMOF (blue), Tb-mesoMOF (red), and 50 μM MP-11 in the HEPES buffer solution (black). (b) Magnified images of Raman band shifts between MP-11 and MP-11@Tb-mesoMOF and (c) between Tb-mesoMOF and MP-11@Tb-mesoMOF.

shifts observed for the other four peaks that are associated with the vibrational modes of the heme structure of MP-11 suggest that MP-11 molecules interact strongly with the framework of Tb-mesoMOF through the heme moieties.

In addition, obvious energy shifts of the Raman bands of Tb-mesoMOF are also observed with the presence of MP-11 within its pores, as shown in Figure 1c.

The four vibrational bands of Tb-mesoMOF at 993, 1056, 1414, and 1613 cm^{-1} are red-shifted to 990, 1054, 1409, and 1610 cm^{-1}, respectively, for MP-11@Tb-mesoMOF. The Raman bands at 993 and 1414 cm^{-1} of Tb-mesoMOF originate from the vibration of triazine of TATB,[14] and the band at 1613 cm^{-1} of

Tb-mesoMOF is assigned to the C=C stretching mode of the benzene ring of the TATB ligand.[15] It is worth noting that the band at 1414 cm^{-1} associated with the vibration of triazine of TATB undergoes a large shift of 5 cm^{-1}, whereas in the case of MP-11 (Figure 1b), the largest band shifts are observed in the peaks at 1317 cm^{-1} (a shift of 6 cm^{-1}) and 1567 cm^{-1} (a shift of 11 cm^{-1}), which are assigned to C−H and C=C of the heme, respectively.[12] This thus suggests that the triazine in the TATB ligand of Tb-mesoMOF interacts strongly with the heme group in MP-11.

These Raman spectroscopic data support a mechanism for MP-11 immobilized inside Tb-mesoMOF (Scheme 1) in which

Scheme 1. Tentative Mechanism for the Specific Interactions between MP-11 and Tb-mesoMOF
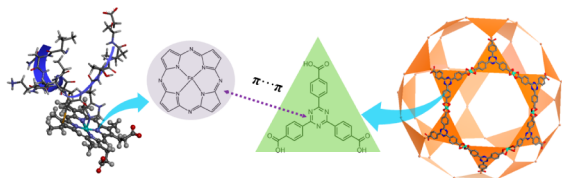
there are strong $\pi\cdots\pi$ interactions between the conjugated systems (including the triazine and benzene rings) of TATB and the heme of MP-11. These strong interactions facilitate retention of the MP-11 molecules inside the cages of the MOFs.

We also measured the Raman spectra for MP-11@MCM-41, which experienced severe leaching during catalytic assays. Figure S3 in the SI shows the Raman spectra of MP-11 and MP-11@MCM-41. Despite the high concentration of MP-11 used during the immobilization process, the Raman signal of MP-11 encapsulated in MCM-41 is much weaker than that in Tb-mesoMOF. This agrees well with the observation that MCM-41 has a much lower loading capacity of MP-11 compared to Tb-mesoMOF.[6a] Two peaks at 1559 and 1636 cm^{-1} that are associated with MP-11 are observed for MP-11@MCM-41, confirming the presence of MP-11 in MCM-41. Interestingly, only the peak at 1640 cm^{-1} in the Raman spectrum was observed to shift position, with a red shift of 4 cm^{-1}, which was also observed for MP-11@Tb-mesoMOF and is due to disruption of the dimer or oligomer structure of MP-11. No additional peak shift was observed for all other bands. These data suggest that there is no strong specific interaction between MP-11 and MCM-41, which should account for the severe leaching of MP-11 during and after its immobilization into MCM-41 (Figure S1 in the SI).

In summary, the interactions between the enzyme and MOF have been unveiled via Raman spectroscopic studies on MP-11@Tb-mesoMOF, in which the MP-11 molecule interacts with the framework of Tb-mesoMOF through $\pi\cdots\pi$ interactions between the heme and conjugated triazine and benzene rings of the TATB ligand. These strong interactions prevent the leaching of MP-11 from Tb-mesoMOF, whereas the lack of specific interactions between MP-11 and the silica material of MCM-41, as also revealed by Raman spectroscopic studies, accounts for the severe leaching of MP-11 from MCM-41. This work thus provides an in-depth understanding of the behavior of the enzyme in solid-state host matrix materials and will be instructive for the design of new functional MOFs for enzyme immobilization to enhance enzyme stability and boost enzyme activity.

■ ASSOCIATED CONTENT

ⓢ Supporting Information

Experimental details and additional Raman spectra. This material is available free of charge via the Internet at http://pubs.acs.org.

■ AUTHOR INFORMATION

Corresponding Authors
*E-mail: xli@usf.edu.
*E-mail: sqma@usf.edu.
Notes
The authors declare no competing financial interest.

■ ACKNOWLEDGMENTS

■ REFERENCES

(1) Schmid, A.; Dordick, J. S.; Hauer, B.; Kiener, A.; Wubbolts, M.; Wtholt, B. *Nature* **2001**, *409*, 258.

(2) Reedy, C. J.; Gibney, B. R. *Chem. Rev.* **2004**, *104*, 617.

(3) Hartmann, M.; Jung, D. *J. Mater. Chem.* **2010**, *20*, 844.

(4) Hanefeld, U.; Cao, L.; Magner, E. *Chem. Soc. Rev.* **2013**, *42*, 6211.

(5) Hartmann, M.; Kostrov, X. *Chem. Soc. Rev.* **2013**, *42*, 6277.

(6) (a) Lykourinou, V.; Chen, Y.; Wang, X.-S.; Meng, L.; Hoang, T.; Ming, L.-J.; Musselman, R. L.; Ma, S. *J. Am. Chem. Soc.* **2011**, *133*, 10382. (b) Chen, Y.; Lykourinou, V.; Vetromile, C.; Hoang, T.; Ming, L.-J.; Larsen, R.; Ma, S. *J. Am. Chem. Soc.* **2012**, *134*, 13188. (c) Chen, Y.; Lykourinou, V.; Hoang, T.; Ming, L.-J.; Ma, S. *Inorg. Chem.* **2012**, *51*, 9156.

(7) Das, R. S.; Agrawal, Y. K. *Vib. Spectrosc.* **2011**, *57*, 163.

(8) (a) Lamontagne, N. D. *Anal. Chem.* **2010**, *82*, 6320. (b) Mo, J.; Zheng, W.; Low, J. J. H.; Ng, J.; Ilancheran, A.; Huang, Z. *Anal. Chem.* **2009**, *81*, 8908. (c) Spiro, T. G.; Smulevich, G.; Su, C. *Biochemistry* **1990**, *29*, 4497.

(9) (a) Procyk, A. D.; Bocian, D. F. *Annu. Rev. Phys. Chem.* **1992**, *43*, 465. (b) Choi, S.; Spiro, T. G.; Langry, K. C.; Smith, K. M.; Budd, D. L.; La Mar, G. N. *J. Am. Chem. Soc.* **1982**, *104*, 4345.

(10) Nijem, N.; Thissen, P.; Yao, Y.; Longo, R. C.; Roodenko, K.; Wu, H.; Zhao, Y.; Cho, K.; Li, J.; Langreth, D. C.; Chabal, Y. J. *J. Am. Chem. Soc.* **2011**, *133*, 12849.

(11) Park, Y. K.; et al. *Angew. Chem., Int. Ed.* **2007**, *46*, 8230.

(12) (a) Stewart, S.; Fredericks, P. M. *Spectrochim. Acta, Part A* **1999**, *55A*, 1615. (b) Frushour, B. G.; Koenig, J. L. *Adv. Infrared Raman Spectrosc.* **1975**, *1*, 35.

(13) (a) Zhang, B. P.; Donohoe, R. J.; Bailey, J. A. *J. Raman Spectrosc.* **2007**, *38*, 410. (b) Zhang, B. P.; Janicke, M. T.; Woodruff, W. H.; Bailey, J. A. *J. Phys. Chem. B* **2005**, *109*, 19547.

(14) Navarro, A.; Lopez Gonzalez, J. J.; Kearley, G. J.; Tomkinson, J.; Parker, S. F.; Sivia, D. S. *Chem. Phys.* **1995**, *200*, 395.

(15) Choi, S.-H.; Park, H. G. *Appl. Surf. Sci.* **2005**, *243*, 76.